

Original Research

Study of Polyaspartic Acid and Chitosan Complex Corrosion Inhibition and Mechanisms

Tengshu Chen^{1,2}, Defang Zeng^{1*}, Saijun Zhou¹

¹School of Resource and Environmental Engineering, Wuhan University of Technology, Wuhan, China

²School of Resource and Environmental Sciences, Quanzhou Normal University, Quanzhou, Fujian, China

Received: 24 July 2017

Accepted: 3 October 2017

Abstract

Polyaspartic acid/chitosan complex (PASP/CS) was synthesized by the reaction of Polyaspartic acid, chitosan, and glutaraldehyde. The graft copolymer (PASP/CS) was characterized by FT-IR. The inhibition corrosion efficiency of the complex was estimated as 83.5%, PASP and only 58.8% when inhibitor concentration was 8 mg/L. PASP/CS is an anodic corrosion inhibitor in Sodium Chloride Solution. The competitive adsorption of chloride ions and PASP/CS in water can form a layer of dense molecular film on the carbon steel surface composite with a non-location effect. PASP/CS combination can effectively inhibit the corrosion in the carbon steel system. The steel surface morphology was analyzed using scanning electron microscopy (SEM) and an adsorption mechanism model is proposed. The high inhibition efficiency of PASP/CS is related to the adsorption of polymer molecules on the steel surface and the formation of a protective film that can successfully inhibit the erosion of corrosive media and prevent the corrosion of carbon steel in the process.

Keywords: polyaspartic acid, chitosan, corrosion inhibition efficiency, adsorption

Introduction

At present there are three primary hazards in industrial water treatment systems: metal corrosion, microbial reproduction, and fouling of heat-exchange equipment. Among these, metal corrosion causes the biggest economic loss, as apart from consumption of a large amount of metals it also causes a huge waste of energy. Metal corrosion causes 10~20% of metal loss every year [1]. In petrochemical and chemical industries, besides economic losses and equipment losses, metal corrosion also leads to a leakage of toxic and harmful

substances, endangering people's health and causing environmental pollution. Therefore, it is extremely crucial to take significant measures to protect metal equipment from corrosion. The addition of a water-treatment agent to industrial metal equipment is a common method for solving the problems of fouling and corrosion in pipes [2-3]. However, currently used water-treatment chemicals do not provide a satisfactory solution and instead cause secondary pollution, seriously hindering their industrial use [4]. Therefore, industries are focusing on the development of environmentally friendly water-treatment chemicals and clean and pollution-free water-treatment systems [5-7].

Polyaspartic acid (PASP) is a green polymer that has no phosphorus and has a good scale and corrosion inhibition ability. Additionally, it has good water solubility and

*e-mail: 316564419@qq.com

biodegradability and hence causes minimal environmental pollution [8-9]. However, a gap still exists between the comprehensive corrosion inhibition performance of PASP and the phosphorus scale inhibitor used in industries [10-12]. Chitosan (CS) is a natural biodegradable biopolymer that is currently the only natural alkaline sugar polymer found in nature, and is an environmentally friendly and renewable resource. However, the inhibition of chitosan has been rarely reported [13-14]. Therefore, it is imperative to conduct further studies on the scale inhibition and corrosion inhibition properties of chitosan and its derivatives. In this study, the complexes of Polyaspartic acid and chitosan were synthesized from polyaspartic acid and chitosan, and their corrosion inhibition performance was analyzed via the rotating hanging plate method. The results were compared with other corrosion inhibitors in water treatment systems such as PASP (polyaspartic acid), PAA (polyacrylic acid), HEDP (hydroxyethylidene two phosphoric acid), HPMA (hydrolyzed polymaleic anhydride), and CS (chitosan). The corrosion inhibition of PASP/CS on carbon steel was studied by the electrochemical method to understand the film formation mechanism and the type of corrosion inhibitor. The state of corrosion resistance on metal surfaces was evaluated with SEM to provide a reliable basis for targeted screening of different production process conditions and water quality.

Experimental

Materials

Polyaspartic acid was supplied by ChangZhou RunYang Chemical Co., Ltd. (Jiangsu, China). Hydrochloric acid, acetic acid, and glutaraldehyde were

supplied by Sinopharm Chemical Reagent Co., Ltd. (Shanghai, China). Anhydrous ethanol, sodium hydroxide and acetone were supplied by Wuhan Huawei Instrument Co., Ltd., (Wuhan, China). Chitosan is from Qingdao Fu Yuan Import & Export Co., Ltd. (Qingdao, China).

602 Constant temperature oil bath pot, RCC-III rotary coupon corrosion tester, JSM-5610LV scanning electron microscope (SEM), CHI660D electrochemical workstation. A3 carbon steel is of the following chemical composition (%): C (0.140), Mn (0.350), Si (0.300), S (0.045), P (0.040), and balance Fe.

Synthesis of Polyaspartic Acid/Chitosan Complex (PASP/CS)

First, add 2 g polyaspartic acid to the beaker, and then add water and stir to make it dissolve; second, take one g chitosan with deacetylation being 80% (molecular weight: 280,000) into a 500-mL three-mouth flask, and add 150 mL 2% hydrochloric acid/acetic acid mixture, and stir it until completely dissolved; third, add the dissolved polyaspartic acid and 2 mL glutaraldehyde aqueous solution with mass fraction being 50%, and adjust its pH value to 6~7 with hydrochloric acid, and then stir the solution to react at the temperature of 40°C. Finally, after the reaction filter the solution by anhydrous ethanol and acetone to get the solid, and then dry it in the drying box to obtain light pink particles, namely complex of polyaspartic acid and chitosan. The reaction is shown in Fig. 1.

Weight Loss Studies for Corrosion Inhibition Efficiency

The corrosion inhibition efficiency of graft copolymer was measured by weight loss of rotating hung steel slices

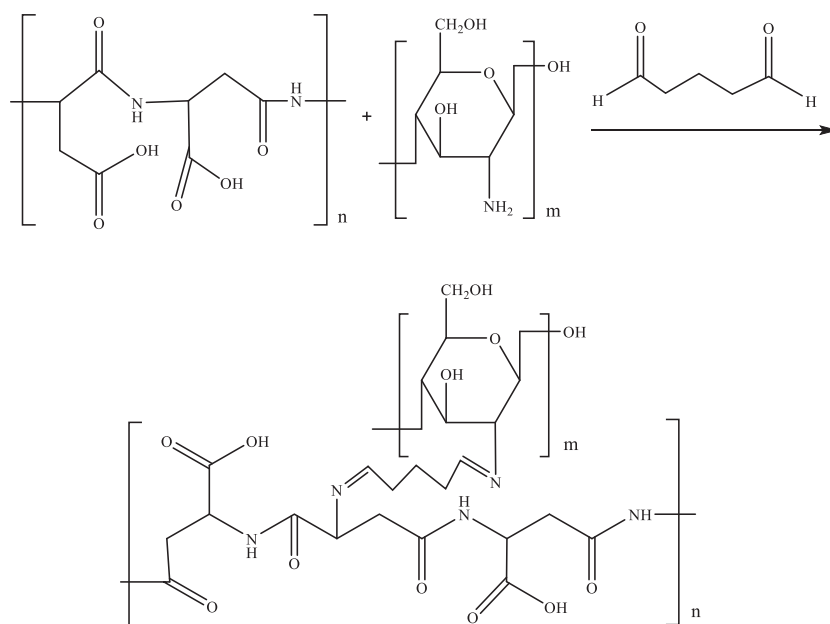


Fig. 1. Synthesis of PASP/CS.

[15]. A3 carbon steel coupon ($50 \times 25 \times 2 \text{ mm}^3$) was used as the corrosion object. The inhibitors were added into the laboratory circulating cooling water. The coupon was placed in the (45 ± 1)°C inhibitor to test the water and was rotated at 75 r/min, which was then removed after 72 h. The blank test without inhibitors was also operated. Corrosion rate v and corrosion inhibition efficiency λ were calculated by using the following equations:

$$v = \frac{8760 \times [(m_0 - m_1) - \Delta m]}{S \times T \times D} \quad (1)$$

$$\lambda = \frac{v_0 - v}{v} \times 100 \quad (2)$$

...where m_0 and m_1 are the mass of carbon steel hung slices before and after the test, Δm is the mass loss of carbon steel hung slices caused by washing in acid, S is the surface area of carbon steel hung slice, T is testing time, D is the density of carbon steel hung slices, v_0 and v are the annual corrosion rates in the absence and presence of scale inhibitor, and λ is corrosion inhibition efficiency.

Electrochemical Test

The instrument used in the electrochemical test is a CHI660D electrochemical workstation (Shanghai Chenhua Instrument Co. Ltd, China). The potential range of impedance test was 10 mV, and frequency range 10 kHz to 10 MHz. The scan rate of Tafel potential test was 0.5 mV/s, and the scanning range was +250 to -250 mV. The test temperature was 25, and test water was 3.5% NaCl solution. The 3-electrode polarization method was used in the experiment. An A3 carbon steel

sheet was used as the working electrode, a saturated calomel electrode (SCE) was a reference electrode, and a platinum sheet was a counter electrode. A3 carbon steel was used for the experimental materials [16-18]. The polarization curves of A3 carbon steel were obtained by using Tafel technology in the 3.5% NaCl solution of the blank and the different concentrations of corrosion and scale inhibitor. Percentage inhibition efficiency (η) was computed from corrosion current density (I_{corr}) values using the relationship as the following Equation (3):

$$\eta = \frac{I_{corr} - I'_{corr}}{I_{corr}} \times 100\% \quad (3)$$

...where in I_{corr} and I'_{corr} are the corrosion current density without and with inhibitor, respectively (mA/cm^2).

Results and Discussion

IR Spectroscopy Characterization of PASP and PASP/CS

FT-IR spectra of chitosan, polyaspartic acid, and polyaspartic acid/chitosan conjugate are shown in Fig. 1. Characteristic peaks assignment of chitosan (Fig. 3a) are the broad band around $3,428 \text{ cm}^{-1}$ attributed to -OH and -NH stretching vibration. The weak band at $2,920$ and $2,867 \text{ cm}^{-1}$ was the characteristic absorbance peak of -CH. The peak at $1,634 \text{ cm}^{-1}$ was ascribed to the amide II band and the C-O stretch of acetyl group. The absorption peak at $1,589 \text{ cm}^{-1}$ was assigned to -NH₂ bending vibration. Additionally, the absorption peaks of symmetric stretching of the C-O-C appeared at $1,157 \text{ cm}^{-1}$, $1,079 \text{ cm}^{-1}$, and $1,026 \text{ cm}^{-1}$ [16]. The IR spectral band of Polyaspartic acid (Fig. 3b) saw characteristic peaks at $3,420$ and $1,601 \text{ cm}^{-1}$, which can be attributed to the stretching and bending vibrations of N-H in amide, respectively. The peak at $1,610 \text{ cm}^{-1}$ was ascribed to C=O, whereas the peak at $1,398 \text{ cm}^{-1}$ corresponds to the strong signal of C-N [19]. As shown in Fig. 3c), compared with chitosan and Polyaspartic acid, new bands at $1,643 \text{ cm}^{-1}$ were ascribed to amide II for PASP/CS, which were also observed. In addition, the peak at $1,589 \text{ cm}^{-1}$ of the primary amine became weak, which meant amino has been partly substituted. The above FTIR analysis clearly indicates that the structure of PASP/CS were confirmed [20].

Analysis of Corrosion Inhibition Performance

In order to study the corrosion inhibition properties of PASP/CS, A3 carbon steel was disposed of in a rotating corrosion tester instrument with (45 ± 1)°C, and the reaction time was 72h. At the end of the experiment, the coupons were removed and dried in the oven after treatment. The corrosion rate was measured by weight

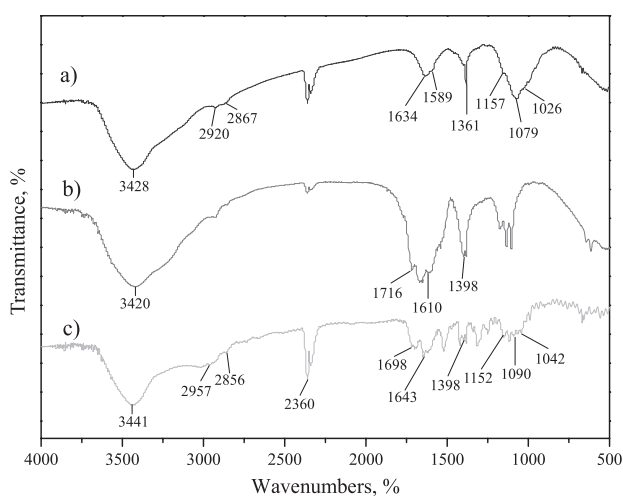


Fig. 2. FT-IR spectra of chitosan a), polyaspartic acid b), and polyaspartic acid-chitosan c).

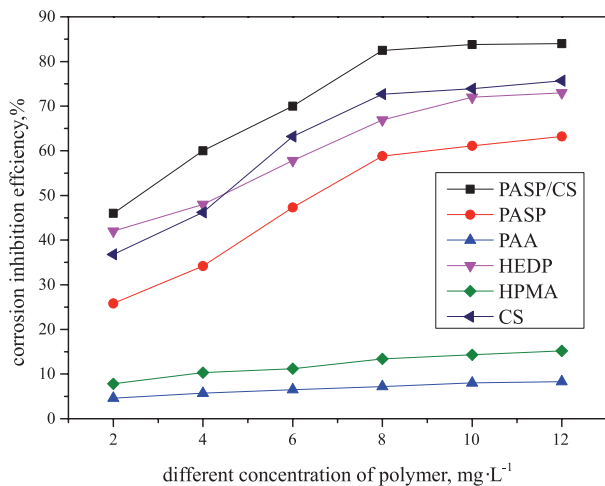


Fig. 3. Influence of different concentrations of polymer on corrosion inhibition.

loss method, and a comparison was made between the results and the commonly used water treatment agents like PASP, HEDP, HPMA, CS, and PAA. The experimental results are shown in Fig. 3.

The corrosion inhibition properties of PASP, HEDP, CS, and PASP/CS increase with the increase of concentration. However, the corrosion inhibition properties of PAA and HPMA did not increase with the increase of concentration, and PAA and HPMA had almost no inhibition. When the concentration was 8 mg/L, the inhibition rates of PASP, HEDP, CS, and PASP/CS were 58.8%, 70.2%, 72.7%, and 83.5%, respectively. The inhibition rate of PASP/CS composite was the highest, which is due to the formation of a corrosion-inhibiting film by the adsorption of amino groups and carbonyl groups in PASP/CS together with the adsorption of hydroxyl groups. At the same time, the polar groups in the composite can enhance the adsorption of metal on the composite, which makes the PASP/CS molecules more concentrated on the metal surface. The hydrophobic groups in the complexes can interact with the hydrophilic polar groups so that the PASP/CS composite forms a compact protective film on the metal surface. The PASP/CS inhibits the diffusion of water and dissolved oxygen to the metal surface by steric hindrance, thereby inhibiting corrosion [21-22].

Influence of pH on Corrosion Inhibition

In order to study the effects of different pH values on the inhibition properties of the PASP/CS composites, the study fixes the PASP/CS dosage at 8 mg/L; puts the treated A3 steel in the (45±1)°C rotation coupon corrosion tester; adjusts pH values respectively at 5, 6, 7, 8, and 9; and sets the reaction time of the experiment at 72 h. At the end of the experiment, remove the coupon and dry it in the oven after treatment, adopt the weight-loss method to measure the corrosion rate, and compare the results with the commonly used water-treatment agents like

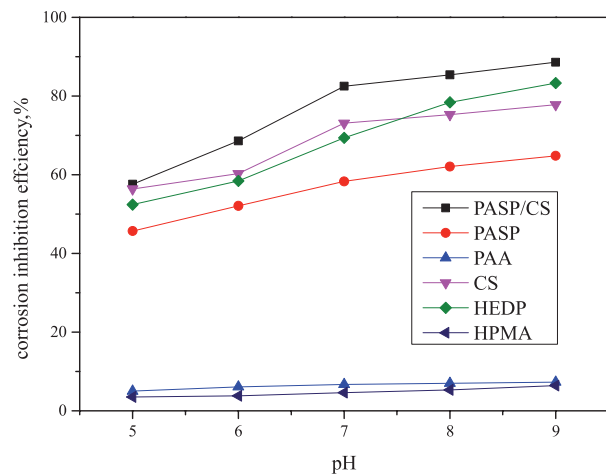


Fig. 4. Effect of pH on corrosion rate.

PASP, HEDP, HPMA, CS, and PAA, which are shown in Fig. 4. As it shows: 1) the corrosion inhibition properties of HPMA and PAA are very poor, which means the pH value has little effect on HPMA and PAA; and 2) the pH value has a significant impact on the corrosion inhibition properties of PASP/CS, PASP, HEDP, and CS: the corrosion inhibition rate of polymers in all groups is not high under acidic conditions, but it improved when pH increased. Compared with the common water-treatment agents, PASP/CS showed better corrosion inhibition performance at the same concentration.

Polarization Curve

A solution-carbon steel system with different concentrations of complexes of polyaspartic acid and chitosan was determined by the electrode polarization curve method. The change of self-corrosion potential and self-corrosion current of carbon steel electrode was analyzed and compared with the electrode polarization curve of carbon steel without adding a composite system. The corrosion inhibition mechanism and corrosion mechanism of PASP/CS composite are studied. The polarization curve test results are shown in Fig. 5. As can be seen from the diagram, the slope of the cathodic and anodic polarization curves of the system increases with the addition of the PASP/CS. Therefore, polarization resistance of the electrochemical reaction also increases. The reaction process of anode and cathode is affected by the electrode surface when the composite is added. As can also be seen from the diagram, the current density of the cathode and anode surfaces of the system decrease as concentration increases, and the corrosion rate also decreases. The change of slope of the Tafel anode is larger than that of the blank solution, but the current of the anode is obvious reduced. However, the change of cathodic polarization curve is very small [23]. Thus, the addition of the PASP/CS compound has great influence on the anodic part of the polarization curve in the experiment, which shows that the PASP/CS is an anodic

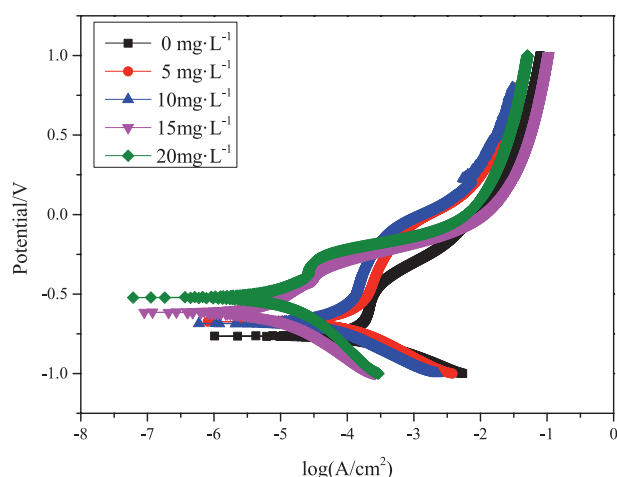


Fig. 5. Polarization curves of carbon steel in different concentrations of PASP/CS.

inhibitor in sodium chloride solution. At the same time, with the increase of the concentration of PASP/CS, the self-decay potential of its polarization curve is moving, and the self-decay current is gradually decreasing. This is due to the competitive adsorption of PASP/CS complexes with chloride ions in water. The composite can form a layer of dense molecular film on the surface of carbon steel by using its non-positioning function, which can effectively inhibit the corrosion of carbon steel by the corrosive medium in the system.

With the Tafel extrapolation method, the corrosion current density of carbon steel electrode with a blank and addition of polyaspartic acid and chitosan complex can be obtained. The electrochemical parameters of the PASP/CS complex at different concentrations can be obtained by fitting the strong polarization region by Fig. 5. The anode slope is b_a , the cathode curve is b_c , and the corrosion current density is i_{corr} ; the corrosion inhibition rate is calculated by Formula 3. It can be seen from Table 1 that the self-corrosion potential of PASP/CS compound is gradually increasing, and the corrosion current density in the system is decreasing gradually. With the increase of the concentration of PASP/CS compound, the corrosion inhibition rate of PASP/CS composite increases gradually. We found that the polarization curve is in agreement with the experimental results.

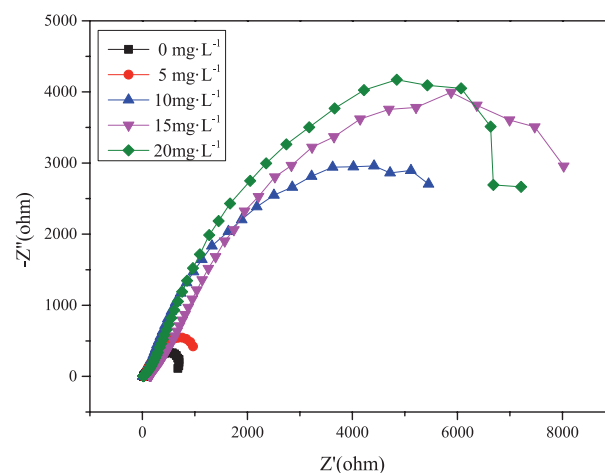


Fig. 6. Nyquist plots for steel in solutions with various concentrations of PASP/CS.

Electrochemical Impedance Spectroscopy

Electrochemical impedance spectroscopy [24-27] not only can rapidly evaluate the corrosion resistance of the inhibitor, but also can obtain various pieces of electrochemical information in the metal film. The high-frequency end of the spectroscopy reflects the information of metal film; the size of the capacitive arc reflects the performance of the metal surface layer dielectric and its shielding properties; the low-frequency end of the spectroscopy reflects the basic information of the metal/solution interface, and the capacitive arc size reflects the transfer process of the dielectric charge in the metal corrosion reaction. Although the inhibitor itself does not participate in the electrode reaction, its adsorption and desorption on the metal surface leads to the change of film coverage, thus affecting the process of electrode reaction. To study the corrosion inhibition mechanism of polyaspartic acid and chitosan composite, polyaspartic acid and chitosan complexes were added into 3.5% sodium chloride solution to measure the electrochemical impedance (Fig. 6). The electrochemical impedance spectroscopy was obtained after adding PASP/CS of different concentrations, and the Bode diagram is shown in Fig. 7.

Table 1. Electrochemical parameters and corrosion inhibition rates of carbon steel in different concentration.

PASP/CS (mg/L)	b_a (V/decade)	b_c (V/decade)	E_{corr} (V)	I_{corr} (mA/m ²)	η (%)
0	9.876	2.832	-0.964	0.1021	
5	11.736	3.155	-0.885	0.0451	55.83
10	12.396	3.187	-0.874	0.0182	82.17
15	15.371	11.874	-0.615	0.0156	84.72
20	16.283	13.811	-0.522	0.0127	87.56

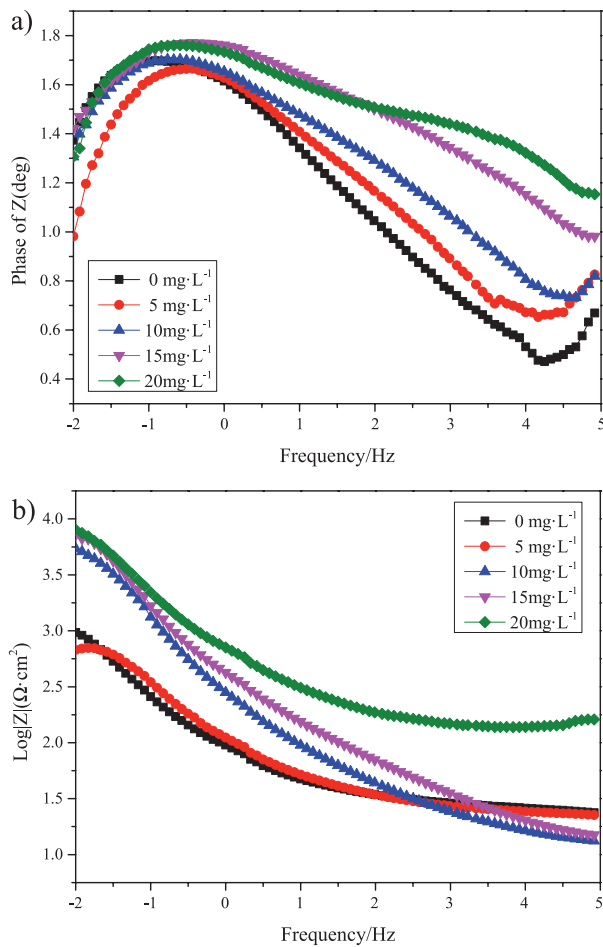


Fig. 7. Bode plots for steel in solutions with various concentrations of PASP/CS.

As can be seen from Fig. 6, the impedance spectrum is semicircular; with the addition of different concentrations of PASP/CS, the resulting impedance spectra have similar characteristics; with the increase of the PASP/CS concentration, the radius of the impedance diagram increases, for the increase of the mixture's concentration makes more PASP/CS complexes deposited on the metal surface, and makes the interaction between the mixture and the metal surface increase, and the electrochemical

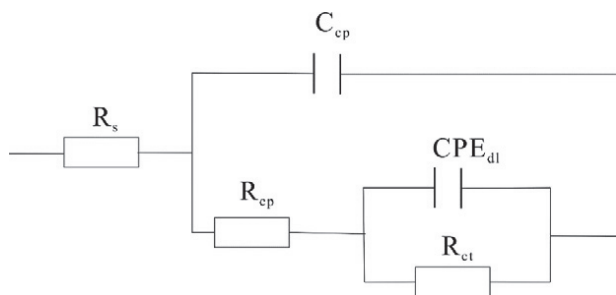


Fig. 8. Equivalent circuit models with various concentrations of electrochemical impedance spectra.

charge transfer process more hindered, thus enhancing the rate of corrosion inhibition. As can be seen from the Bode diagram: there are two time constants in the high-frequency and low-frequency regions, with the increase of the complex concentration, the peak of phase angle is also gradually increasing and moves slowly to the low-frequency region, which indicates that the PASP/CS composite forms a strong adsorption layer on the electrode surface, which makes the resistance of electrode reaction increase, and the progress of corrosion reactions impeded [28].

According to the EIS and the Bode diagram, the equivalent circuit diagram as shown in Fig. 8 is established. In the figure, R_{cp} represents the impedance value of solution and corrosion product interface during the dissolution process, R_s indicates the resistance of the electrolyte, and R_{ct} represents the associated charge transfer resistance of the metal and the interface of the corrosion product. C_{cp} represents the capacitance of the corrosion product associated with the dissolution process of the dissolved interface and CPE_{dl} is the constant phase angle element between the corrosion product and the metal interface. The equivalent circuit is used to fit the parameters, and the results are shown in Table 2. The R_{ct} value increases with the increase of the PASP/CS concentration, indicating that the amount of PASP/CS adsorbed on the carbon steel surface is also increasing, thus making the corrosion resistance increase and the CPE_{dl} and the C_{cp} gradually be reduced. This is due to the adsorption of PASP/CS on the surface of carbon steel: the PASP/CS molecule replaces the water molecule layer to be adsorbed on the surface of the metal, and the dielectric constant of the composite is smaller than that of the water molecule, so the adsorption of the PASP/CS reduces the interfacial capacitance of the metal.

SEM Pictures of Carbon Steel in the Absence and Presence of PASP/CS

In order to study the corrosion inhibition mechanism of PASP/CS on carbon steel, carbon steel coupons were used in the 3.5% sodium chloride solution without PASP/CS and with 10 mg/L PASP/CS, the reaction time was 72 hours. At the end of the experiment, the coupons were taken out to be cleaned with anhydrous ethanol and acetone and then dried. The surface corrosion of PASP/CS on carbon steel was analyzed by a JSM-5610LV electron microscope. After scanning, the morphology was magnified 200 and 2,000 times. The results are shown in Fig. 9 for the surface morphology of carbon steel in solution with and without PASP/CS. As can be seen from the diagram, carbon steel (A1 and A2) treated without PASP/CS composites are seriously corroded and form deeper pits on the surface. This is because the carbon steel coupons were exposed in aqueous solution with high chloride ion, which can penetrate into the surface of carbon steel and cause corrosion on its surface [29]. When the complex of polyaspartic acid and chitosan was added, the corrosion morphology of carbon steel surface (B1 and

Table 2. Simulative electrochemical parameters for steel in solutions with various concentrations of PASP/CS.

C(mg/L)	$R_s(\Omega \cdot \text{cm}^2)$	$R_{ct}(\Omega \cdot \text{cm}^2)$	$\text{CPE}_{dl}(\mu\text{F} \cdot \text{cm}^{-2})$		$C_{ep}(\mu\text{Fcm}^{-2})$	R_{cp}
			$Y_{dl}(\Omega^{-1}\text{cm}^{-2}\text{s}^n10^{-6})$	n_{dl}		
0	13.03	11.39	3.14	0.78	1.571	4.837
5	13.18	20.55	2.16	0.74	1.067	10.384
10	16.13	38.52	1.7	0.67	0.382	17.359
15	20.37	63.89	1.69	0.65	0.183	20.482
20	24.1	81.46	1.32	0.67	0.0847	23.743

B2) was regular. From the electron microscope diagram magnified 200 and 2,000 times, we can see that carbon steel coupons B1 and B2 do not have pits on the surface as A1 and A2 do, and the metal surface is regular. We can conclude that the PASP/CS composite forms a compact protective film on the surface, thus preventing the surface corrosion of carbon steel.

Conclusion

Polyaspartic acid/chitosan complex (PASP/CS) was synthesized by the reaction of polyaspartic acid, chitosan, and glutaraldehyde. Through the research on its performance, the PASP/CS combination can effectively inhibit corrosion in the carbon steel system. PASP/CS is found to have better corrosion inhibition performance than the commonly used water-treatment agents. Polarization curves show that PASP/CS is an anodic inhibitor in sodium chloride solution. PASP/CS can be adsorbed on the surface of carbon steel and forms a strong adsorption layer on the electrode surface, which resists the increase of electrode reaction, thus hindering the corrosion reaction. SEM indicated that the high inhibition efficiency was in terms of adsorption of inhibitor molecules and protective film formation on the metal surface.

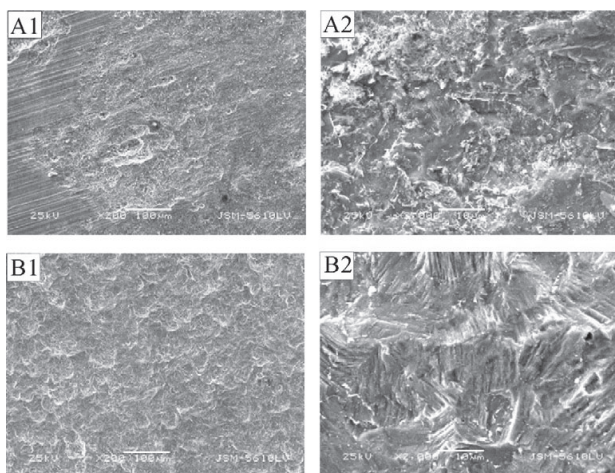


Fig. 9. Scanning electron microscope on the surface of carbon steel without PASP/CS(A1, A2) and with PASP/CS (B1, B2).

Acknowledgements

This research was financially supported by the Ministry of Education in China Project of Humanities and Social Science (No. 13YJCZH276).

References

1. WANG P. Wastewater reuse and circulating cooling water treatment technology in thermal power plant. China Electric Power Press: Beijing, China, 32, **2013** [In Chinese].
2. WANG W., YIN X.P., LING C. Preparation and capacity evaluation of corrosion and scale inhibitors which are environment-friendly and free of phosphorus. *Industrial Water Treatment.*, **30** (1), 16, **2010** [In Chinese].
3. LI S.Y., WANG G., SHAO B. Research on aging inhibiting corroding and scaling properties of green water treatment agents for A20. *Cleaning World.*, **27** (1), 9, **2011** [In Chinese].
4. CHEN W., SHU P.L., TIAN D.L. Calcium carbonate inhibition by a phosphonate-terminated poly(maleic-cosulfonate) polymeric inhibitor. *Desalination.*, **249** (1), 1, **2009**.
5. LOW K.C., WHEELER A.P., KOSKAN L.P. Green chemistry applied to corrosion and scale inhibitors. *Adv Chem Ser.*, **248**, 99, **1996**.
6. NAKATO T., YOSHITAKE M., MATSUBARA K., TOMIDA M. Relationship between structure and properties of polyaspartic acids. *Macromolecules.*, **31** (7), 2107, **1998**.
7. KOSKAN L.P. Polyaspartic acid as a calcium sulfate and a barium sulfate inhibitor. US 5116513, **1992**.
8. QIF, SHANG P., YANG Y. The Research Progress of Green Polymer Polyaspartic Acid. *Hebei Chemical Engineering and Industry.*, **33** (6), 14, **2010**[In Chinese].
9. ZHAO Y.S., LI Q., HU D., SHI H.G., JIA Z.X., CHEN X.L. Synthesis and Responsive Properties of Modified Poly (Aspartic acid) /Poly (Acrylic acid) Composite Absorbent Resin. *FINE CHEMICALS.*, **36** (9), 620, **2016** [In Chinese].
10. GAO Y.H., LIU Z.F., ZHANG L.H., LI H.H., GAO M.L. Study on the capacity of polyaspartic acid copolymer for calcium phosphate inhibition. *Industrial Water Treatment.*, **36**, 63, **2016** [In Chinese].
11. BINGRU Z., HE C. J., WANG C., PEIDI S., LI F.T., LIN Y. Synergistic corrosion inhibition of environment-friendly inhibitors on the corrosion of carbon steel in soft water. *Corrosion Science.*, **94** (7), 6, **2015**.
12. HAN Y.F., DUAN G.Q., WU F.L., CHEN L., ZHANG J.J., ZHOU Y.Z. Latest Research Progress of Environmentally Friendly Corrosion Inhibitors. *Total Corrosion Control.*, **30** (5), 57, **2016** [In Chinese].

13. CHANG S.H., VICTOR LIN H.T., WU G.J., GUO J.T. pH Effects on solubility, zeta potential, and correlation between antibacterial activity and molecular weight of chitosan. *Carbohydrate Polymers.*, **134**, 74, **2015**.
14. DEMADIS K.D., PREARI M. "Green" scale inhibitors in water treatment processes: the case of silica scale inhibition. *Desalination and Water Treatment.*, **3** (55), 749, **2015**.
15. TOUIR R., CENOUI M., EIBAKRI M., TOUHAMI M. Sodium gluconate as corrosion and scale inhibitor of ordinary steel in simulated cooling water. *Corros. Sci.*, **50**, 1530, **2008**.
16. KUBOTA N., EGUCHI C., FACILE Y. Preparation of water-soluble N-acetylated chitosan and molecular weight dependence of its water-solubility. *Polymer Journal.*, **29** (2), 123, **1997**.
17. MIGAHED M.A., AL-SABAGH A.M., KHAMIS E.A., ZAKI E.G. Quantum chemical calculations, synthesis and corrosion inhibition efficiency of ethoxylated [2-(2-{2-[2-(2-benzenesulfonylaminoethylamino)-ethylamino]-ethylamino}-ethylamino)-ethyl]-4-alkylbenzenesulfonamide on API X65 steel surface under H₂S environment. *Journal of Molecular Liquids.*, **212**, 360, **2015**.
18. PATRICIA A.O., BEEMA J.T., JUDE O.I. Thermo-mechanical and corrosion inhibition properties of graphene/epoxy ester-siloxane-urea hybrid polymer nanocomposites. *Progress in Organic Coatings.*, **88** (12), 237, **2015**.
19. LI J.Y., AO Y.B., ZENG D.F. Study on synthesis and inhibition performance of PASP. *Appl. Chem. Ind.*, **37**, 770, **2008**.
20. SANTOSH K., JOONSEOK K., HYERIM M., GUTPA M.K., DUTTA P.K. A new chitosan-thymine conjugate: Synthesis, characterization and biological activity. *International Journal of Biological Macromolecules.*, **50**, 493, **2012**.
21. ABDEL A.M., NABEY B. A., KHAMIS D. E., ABD E.K. A natural extract as scale and corrosion inhibitor for steel surface in brine solution. *Desalination.*, **27**, 337, **2011**.
22. SANGEETHAY., MEENAKSHIS., SAIRAMSUNDARAM C. Corrosion mitigation of N-(2-hydroxy-3-trimethyl ammonium) propyl chitosan chloride as inhibitor on mild steel. *International Journal of Biological Macromolecules.*, **72** (5), 1244, **2015**.
23. CHEN T., TAN T., HUANG W.L., YI B., YUAN X.J., ZHANG J.X. Polarization Curve Measurement of Corrosion Rate of Hot-dipped Component in Transmission Equipment and Parameter Optimization. *CORROSION & PROTECTION.*, **35** (2), 120, **2014** [In Chinese].
24. HMAMOU D., SALGHI R., ZARROUK A., ZARROK H., TOUZANI R., HAMMOUTI B., ASSYRY A.E. Investigation of corrosion inhibition of carbon steel in 0.5 M H₂SO₄ by new bipyrazole derivative using experimental and theoretical approaches. *Journal of Environmental Chemical Engineering.*, **3** (6), 2031, **2015**.
25. YADAV M., SINHA R.R., KUMAR S., BAHADUR I., EBENSO E.E. Synthesis and application of new acetohydrazide derivatives as a corrosion inhibition of mild steel in acidic medium: Insight from electrochemical and theoretical studies. *Journal of Molecular Liquids.*, **20** (8), 322, **2015**.
26. MASOUMEH M., SONG Z.L., TAO X. Introducing a novel bacterium, *Vibrio neocaledonicus* sp., with the highest corrosion inhibition efficiency. *Electrochemistry Communications.*, **51** (9), 64, **2015**.
27. NNABUK O., EDDY H., MOMOH E., EMEKA O. Theoretical and experimental studies on the corrosion inhibition potentials of some purines for aluminum in 0.1 M HCl. *Journal of Advanced Research.*, **6** (2), 203, **2015**.
28. SHI D.L. Preparation and inhibition performance of the vanillyl-chitosan quaternary ammonium salts. *Ocean University of China.*, **2014**.
29. DEFLORIAN F., ROSSI S., FEDEL M., ECCO L.G., PAGANICA R., BASTAROLO M. Study of the effect of corrosion inhibitors on powder coatings applied on steel. *Progress in Organic Coatings.*, **10** (77), 2133, **2014**.